Experimental Study on the Influence of *n*-butanol blending on the Combustion, Autoignition and Knock Properties of Gasoline and its Surrogate in a Spark Ignition Engine.

E. Agbro[1], W. Zhang[2], A. S. Tomlin[1], A. Burluka[3]

[1]School of Chemical and Process Engineering, University of Leeds, Leeds, UK.
[2]School of Mechanical Engineering, University of Leeds, Leeds, UK.
[3]Faculty of Engineering and Environment, Northumbria University, Newcastle, UK.

Abstract

The impact of *n*-butanol blending on the combustion, autoignition and knock properties of gasoline has been investigated under supercharged spark ignition engine conditions for stoichiometric fuel/air mixtures at intake temperature and pressure conditions of 320 K and 1.6 bar, respectively, for a range of spark timings. A toluene reference fuel (TRF) surrogate for gasoline containing toluene, *n*-heptane and iso-octane has been tested experimentally in the Leeds University Ported Optical Engine (LUPOE) alongside a reference gasoline and their blends (20 % *n*-butanol and 80 % gasoline/TRF by volume). Although the gasoline/*n*-butanol blend displayed the highest burning rate, and consequently the highest peak pressures compared to gasoline, TRF and the TRF/*n*-butanol blend, it exhibited the least propensity to knock, indicating that addition of n-butanol provides an opportunity for enhancing the knock resistance of gasoline as well as improving engine efficiency via the use of higher compression ratios. The anti-knock enhancing quality of *n*-butanol on gasoline was however observed to weaken at later spark timings. Hence, whilst *n*-butanol has shown some promise based on the current study, its application as an octane enhancer for gasoline under real engine conditions may be somewhat limited at the studied blending ratio. As expected based on previous ignition delay studies, the TRF showed an earlier knocking boundary than the rest of the fuels, which may possibly be attributed to the absence of an oxygenate (ethanol or *n*-butanol) as present in the other fuels and a lower octane index. Overall, the TRF mixture gave a reasonable representation of the reference gasoline in terms of the produced knock onsets at the later spark timings for the pure fuels. However, on blending, the TRF did not reproduce the trend for the gasoline at later spark timings which can be linked to difficulties in capturing the temperature trends in ignition delays around the negative temperature coefficient region observed in previous work in a rapid compression machine (Agbro et al., Fuel, 2017, 187:211-219).

Keywords: *n*-butanol, autoignition, spark ignition engine, knock onsets.

1.0 Introduction

Engine downsizing, which involves the use of a smaller engine that provides the power of a larger engine, is currently being explored by engine designers to improve fuel efficiency and, consequently, emissions performance. In order to provide a more fuel-efficient downsized engine with similar performance to a larger engine, a turbocharger or supercharger is usually required to increase the density of the inlet air. However, supercharging and the use of high compression ratios are currently limited by the problem of engine knock.[1] There is therefore a strong interest in using fuel components with high anti-knock qualities as blending agents (octane boosters)[1] as well as a renewed drive, within the research community, to better understand the autoignition and knock behaviour of alternative fuels for the purpose of optimising engine design and control strategies. Bio-derived alcohols are considered as viable blends for petroleum derived fuels due to their potential to improve the octane and emission performance of fossil-derived fuels.[2] The similarity of their physical and chemical properties to those of fossil-derived fuels make them compatible with modern engines, particularly when used in blends.[2, 3] This means that fewer modifications have to be made to existing hardware, and additional costs for infrastructure and maintenance can be lower than for other biofuels. Ethanol has been used extensively and can be used at low blending ratios with gasoline without requiring engine modifications. Butanol isomers have been less commonly used in practice, but may offer the potential for higher blending ratios due to better similarity of their properties to gasoline than ethanol.

In a spark ignition (SI) engine, combustion is initiated towards the end of the compression stroke with the spark discharge from a spark plug. Once the fuel air mixture around the spark plug is ignited by the spark, a flame kernel is formed and it gradually evolves until it becomes a fully developed self-sustaining premixed flame front. The latter propagates across the entire combustion chamber volume[4-7] compressing the unburned mixture ahead of it to higher temperatures and pressures. Under normal non-knocking combustion, the unburned mixture (the end gas) is completely consumed by the advancing flame front before the chemical reactions in the end gas are able to develop to the point where autoignition occurs. Under abnormal (knocking) combustion, the advancing flame front together with the moving piston, compresses the end gas to high pressure and temperature (*P-T)* conditions sufficient to accelerate the chemical reactions in the end gas at locations remote from the spark plug so that a spontaneous ignition (autoignition) of the end gas occurs.[8] Following the autoignition and

rapid consumption of the end gas, sonic pressure waves are generated from the autoignition spot which further interact with the flame front to produce very high frequency pressure oscillations within the engine cylinder.[8] The resulting high pressure oscillations impinge on the engine cylinder walls causing vibration and a sharp audible (pinging) sound generally referred to as knock.[4] Engine knock is a highly undesirable combustion phenomena because, apart from the discomfort it brings to vehicle drivers and passengers, it can lead to serious damage of the engine hardware and loss of power.

While a number of engine studies investigating the pollutant emissions of *n*-butanol and ethanol blended with gasoline have been reported,[9-17] only a very limited number of such studies have addressed the autoignition and knock onsets of the above alcohols when blended with gasoline.[18-21] Moreover, research investigating the influence of the particular biofuel *n*-butanol on the autoignition and knock properties of gasoline under well-controlled supercharged engine conditions applicable to modern downsized engines are rare, and this provides a stimulus for the present work. Wider penetration and sensible use of biofuels and their blends with gasoline in internal combustion engines requires a thorough understanding of their properties and the effect of their use in terms of their autoignition and knock behaviour under a wide range of conditions. This could be effectively realised through computer modelling and analysis, were accurate representation of the fuel oxidation processes to be possible within practical engine models. Because gasoline composition is complex, a surrogate is required to represent gasoline within the context of computer modelling when investigating it either in isolation or under blending with bio-derived alcohols.[22, 23] Therefore, a major question that needs to be answered is whether a surrogate mixture of only a few components may accurately represent the autoignition and knock behaviour of a typical complex research grade gasoline. Therefore, in this work, a surrogate developed to represent a complex gasoline has been tested in isolation, as well as under blending with *n*-butanol under well-controlled conditions in the Leeds University Ported Optical Engine (LUPOE). Results are compared with neat gasoline thus deriving data sets for the autoignition and knock of gasoline and a gasoline/*n*-butanol blend for model validation and improvement. The experiments studying the impact of *n*-butanol blending on the combustion, autoignition and knock properties of gasoline were carried out in the LUPOE under supercharged conditions for stoichiometric fuel-air mixtures at intake temperature and pressure conditions of 320 K and 1.6 bar, respectively, for a range of spark timings of 2 °CA- 8 °CA bTDC (crank angle degrees before the top dead centre). The evaluation

of a chemical kinetics model for the blends is also presented in a companion paper of this Special Issue through simulation of the experimental results reported here.

2.0 Methodology

2.1 The LUPOE-2D research engine

The Leeds University Ported Optical Engine, Mk II with a Disc-shaped combustion chamber (LUPOE-2D) developed by Roberts and Sheppard[24] was used for acquiring all engine data presented in this work. The LUPOE-2D engine is a single cylinder research engine with uniform in-cylinder turbulence in the combustion chamber. The overhead train system was replaced with two diametrically opposed rectangular intake ports to allow for full-bore optical access. The dimensions and inclination of the ports were chosen so as to minimise large-scale flow features such as swirl and tumble. The exhaust gases are purged through two rings of circular exhaust holes drilled around the liner, see Figure 1. In order to control the charge composition and avoid dilution with trapped residual exhaust gases, the engine is operated in a skip-firing mode with the cylinder flushed with fresh mixture during the cycles with skipped ignition. While LUPOE has a full-bore top quartz window (Figure 1) for high speed filming, in this work a metal blank was used instead of quartz for all experiments since the focus was on investigating engine knock at high pressures entailing the risk of damaging the optical head. A spark plug located in the centre of the cylinder head was employed for igniting the fuel mixture. The main specifications of LUPOE-2D are given in Table 1 while a cross sectional view of the engine is shown in Figure 1.

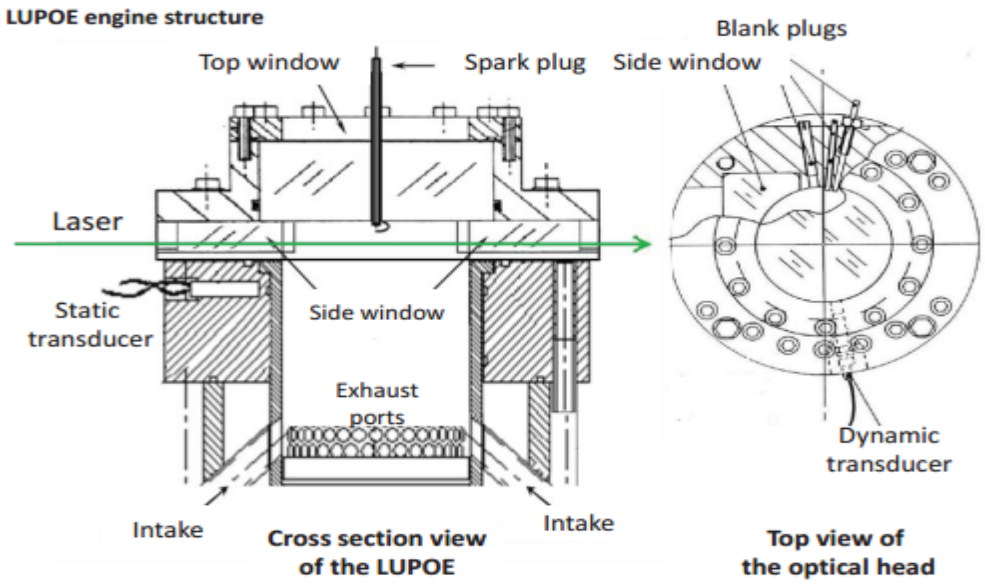

Figure 1. A cross sectional view of LUPOE-2D and a top view of the optical head.[25]

Table 1. LUPOE-2D design specifications. Adapted from Ling.[25]

Bore (mm)	80
Stroke (mm)	110
Clearance height (mm)	7.5
Connecting rod length (mm)	232
Compression ratio	11.5
Intake ports opening/closure (^{0}CA aTDC)	107.8
Exhaust ports opening/closure (^{0}CA aTDC)	127.6
Number of exhaust ports	15

2.2 Fuel and air supply

LUPOE-2D is designed to operate under supercharged conditions where air is supplied to the intake ports from a high pressure compressed air line. The fuel was mixed with the air through a bespoke fuel injector located at the middle of a Venturi meter positioned about 350 mm upstream of each intake port. The mass flow rate of the fuel was controlled with a Series M53 Bronkhorst Coriolis mass flow controller accurate to 0.1% of the reading. Before using a different fuel mixture, the mass flow controllers and fuel lines were thoroughly purged with pressurised air for about half an hour in order to remove all traces of the previous fuel and to avoid charge contamination. Subsequently, the new fuel was allowed to flow from the fuel tank across the fuel lines for about a minute to remove any leftover of fuel residues. A series of five 175 W band heaters and one 200 W band heater positioned along the length of the intake were employed to raise and maintain the temperature of the intake air. The heat supplied to the air enabled the air-fuel mixture to evaporate completely before entering the combustion chamber. Heating of the cylinder barrel and head was accomplished with the help of several 50 W cartridge heaters equally spaced around the barrel. The temperatures were monitored and controlled by thermocouples positioned in the cylinder barrel just upstream of the intake port with readings processed by a Digitron 4801 control unit. In this work, all experiments were performed with the temperature of the intake set to 50 °C.

2.3 Engine control and data acquisition system

The control system employed in LUPOE was a bespoke control system designed and implemented by Ling.[25] It comprised a micro controller DsPIC6014A which represents the core of the control system and a microchip MPLAB ICD 3 in-circuit debugger system used for debugging and programming the microcontroller. The coding and debugging of the microcontroller was made possible with the help of the MPLAB integrated development environment (IDE) software tools. The microcontroller reads the TDC signal and shaft encoder clock signals and controls ignition, valve operation timing, and the start and end of the data acquisition period.

The in-cylinder pressure was measured using two types of pressure transducers. One is a Kistler piezoelectric pressure transducer Type 601A which is a dynamic pressure transducer used for measuring rapidly changing pressures in the engine cylinder due to its high response rate. The dynamic pressure transducer was mounted flush to the cylinder wall with only the diaphragm exposed to the chamber volume. A Kistler charge amplifier Type 5007 was employed to transform the output charge of the dynamic pressure transducer into potential difference. A reference pressure was provided for the dynamic pressure by a Kistler absolute pressure transducer, type 4045A20, located at the lower end of the piston barrel where it measured the pressure during the initial phase of compression. The location of the absolute pressure transducer levels with the piston crown at 60 °CA bTDC when the pressure is normally between 0.25 - 0.3 MPa is chosen so that the absolute pressure transducer is protected from the high temperatures and pressures experienced during the latter part of the compression and combustion stages. The signal from the absolute pressure transducer is amplified using a Kistler Series 4601A piezo-resistive amplifier. In-cylinder pressure data were sampled at a resolution of 0.2 °CA triggered by 1800 output pulses produced by the shaft encoder per revolution; no correction was made for varying piston speed in different parts of stroke. All experimental data were recorded using a data acquisition system comprising two NI Peripheral Component Interconnect (PCI) cards and a personal computer (PC) running LabVIEW. Dynamic and absolute pressure analogue signals were connected to two different channels of National Instruments 6110 analogue PCI card to convert the signals to digital form while digital signals (TDC, BDC etc.) were recorded by a NI DIO-32HS digital PCI card. Re-sampling of the original data with respect to crank angle was accomplished with the help of a MATLAB code. The raw pressure data was cut into

individual cycles using the BDC signal location as the reference point, allowing both the firing cycles and motoring cycles to be identified. The effect of noise in the analogue pressure signals of each firing cycle was eliminated using a low pass 2nd order Butterworth filter with a cut-off frequency of 2 KHz, while the built in-MATLAB function 'filfilt' was subsequently applied to ensure a zero phase shift. The peak pressure of each firing cycle is given by the maximum value of the pressure cycle filtered by a low-pass filter. When the low pass filter was not applied, it was therefore possible to identify the condition under which knock was present.

2.4 Fuels and test procedure

A total of four fuel mixtures, tested previously in the Leeds RCM[26] were also tested in the current experiments using LUPOE-2D. These included a reference commercial gasoline of research octane number (RON) 95, a toluene reference fuel (TRF), a blend of 20 % by volume of *n*-butanol with 80 % by volume of RON95 gasoline referred to as ULGB20 and a blend of 20 % by volume of *n*-butanol with 80 % by volume of TRF (TRFB20). The TRF mixture was used as a simple surrogate of known composition, formulated to represent the complex gasoline in chemical kinetic modelling of the autoignition behaviour of gasoline and its blend with *n*-butanol under practical engine conditions. The methodology used in formulating the TRF surrogate is described in Agbro et al.[26]. There are a number of properties relevant to combustion in engines, such as air-fuel ratio (AFR), calorific value, laminar and turbulent flame speed and ignition delay at p-T conditions of the fresh gas. Using a three-component surrogate, only three properties can be matched. Here, RON is taken as a proxy measure of ignition delays and H/C ratio as parameter to characterise energy release and AFR. Comparisons of turbulent flame speeds can be performed *a posteriori* as will be discussed later in the paper. The components and composition of the reference gasoline, supplied by Shell Global Solutions, are given in Table 2 under reference PRF801a, alongside the composition of the formulated TRF surrogate. The various properties of the reference gasoline and the formulated surrogates such as the RON, motor octane number (MON), hydrogen-carbon ratio (H/C) etc., as well as the calculated composition of the blended surrogate can be found in Agbro et al.,[26] and selected properties are repeated here in Table 2.

Table 2. Comparison of the composition and properties of reference gasoline and formulated 3-component surrogate

Gasoline component	**PR5801**[a]	**TRF95**	**TRF95**	**TRF95**
	% volume	**Component**	**% mole**	**% volume**
Paraffins	47.1	Iso-octane	57.50	65.64
		n-heptane	11.25	11.40
Olefins	7.9	-	-	-
Naphthenes	8.2	-	-	-
Aromatics	26.0	Toluene	31.25	22.97
Oxygenated (ethanol)	4.7	-		
RON	95		95	
MON	86.6		89.8[b]	
H/C	1.934		1.934	
S=RON-MON	8.4		5.2	
OI	108.6[c]		103.4[c]	

[a] Values are taken from analysis supplied by Shell Global Solutions
[b] Calculated based on a linear blending law and component properties
[c] Calculated using equation (1)

Throughout the experiments, LUPOE-2D was operated at a speed of 750 RPM at an initial charge temperature of 323 K, a pressure at the beginning of the compression stroke of 1.6 bar and an equivalence ratio of 1. These conditions can be interpreted using an effective octane number known as the octane index (*OI*) pioneered by Kalghatgi[27] as an empirical extrapolation of standard fuel test results to modern strongly supercharged engines:

$$OI = (1 - K) \cdot RON + K \cdot MON = RON - KS \quad (1)$$

where S = RON- MON is the sensitivity of the fuel and the engine dependent parameter K is determined from the charge temperature T_{15} at which the pressure in the compression stroke reaches 15 bar:

$$K = 5.6 \cdot 10^{-3} T_{15} - 4.68 \quad (2)$$

The temperature in the compression stroke for the present experiments was calculated taking into account the heat losses to the cylinder walls[28] as shown in Figure 2. For the present conditions, for all four fuels $T_{15} = 547 \pm 1K$ and, as is common for strongly charged engines

with charge cooling, Eq. (1) yields a rather large negative factor $K = -1.62$ and *OI* values for both fuels that are greater than the RON and MON values. In matching the RON and H/C values of the reference gasoline with only 3 surrogate components, small discrepancies in *S* and therefore in the calculated *OI* values for the TRF compared to PR5801 are observed.

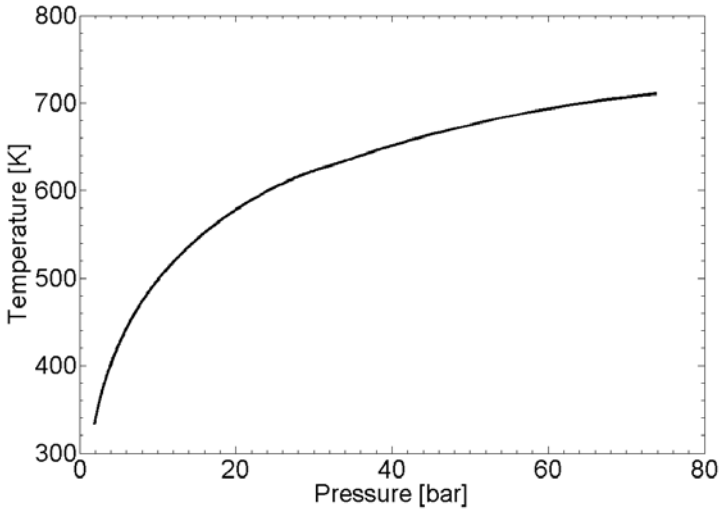

Figure 2. The unburnt charge temperature vs. pressure with account of heat losses.

A combination of a skip firing ratio of 20 and 14 fuelling cycles (i.e. fuel was not injected in 6 of the cycles) was found to produce autoignition free operation during the compression phase, while also allowing cylinder volume to be properly purged of exhaust gas residues from the firing cycle. The spark timing was gradually advanced by 1 °CA beginning from 2 °CA bTDC until the knock boundary was identified. The knock boundary was taken as the spark timing at which knock occurred in over 90 % of the total firing cycles.[25] The knock boundaries so determined were: 6 °CA bTDC for gasoline, the gasoline/*n*-butanol blend and the TRF/*n*-butanol blend, but only up to a limit of 4 °CA bTDC for TRF. The spark timing was further advanced above the knock boundary until the peak pressure recorded in the cylinder was within the allowable peak pressure limit of 120 bar which the cylinder head is able to withstand.

Across the range of spark timings investigated for each fuel mixture and set of tests, knocking cycles were identified by listening to the audible pinging sound caused by impact of the pressure waves on the piston (audible detection by the ear alone) and from the recorded pressure traces. The data acquisition system allowed a continuous registration of 13 firing cycles in a row. Strong knock occasionally led to an increase of the engine wall temperature

requiring interruption to bring it back to normal. Overall, a total of three series or 39 firing cycles were captured for each set of conditions.

2.5 Determination of autoignition and knock in LUPOE-2D

The knock properties of a fuel mixture undergoing combustion in an engine can be characterised using two key properties namely, the knock onset and knock intensity.[29] In this study, the method described in Liu[30], was employed to determine the knock onset location and knock intensity from measured in-cylinder data.

As illustrated in Figure 3, the knock onset position is given by the first prominent point of inflection on the measured pressure trace which leads further into a series of pressure fluctuations. The point of inflection is determined by computing the rate of change of the pressure gradient with crank angle travelled (θ) over any three points on the pressure data using the equation to give the knock onset (*KN*) in CA degrees:

$$KN = -\frac{d^2P}{d\theta^2} = \frac{2P_n - P_{n-1} - P_{n+1}}{\Delta\theta^2} \quad (3)$$

where P_{n-1}, P_n, P_{n+1} are three consecutive values of the recorded pressure. The knock onset was finally identified by scanning through the values of *KN* until a preset threshold was exceeded. The knock intensity in this method is given by the maximum amplitude of the pressure rise rate.

Selecting a single threshold value for all engine conditions could potentially lead to large errors in identifying the correct knock onset location due to the inherent problem of cyclic variability in engine pressure data. After an initial visual inspection of the knock pressure oscillations for all knocking conditions, a varying threshold value in the range of 20 – 30 bar/CA^2 was chosen in order to identify the knock onset location.

According to Ling[25] knock happens later than the point of the onset of autoignition. In his work, combustion imaging from a fast camera was used to distinguish between the two by superimposing and comparing both the autoignition onset detected by imaging, with the simultaneously recorded knocking pressure trace, and a systematic crank angle difference between the two events was about 0.2 °CA which is deemed to be negligible for the present work. Since the study of combustion using imaging was not used in this work, and since autoignition onset is the key parameter being predicted in the related simulations, the knock

onset calculated from the pressure data was considered to be the same as the instant of the end-gas self-ignition.

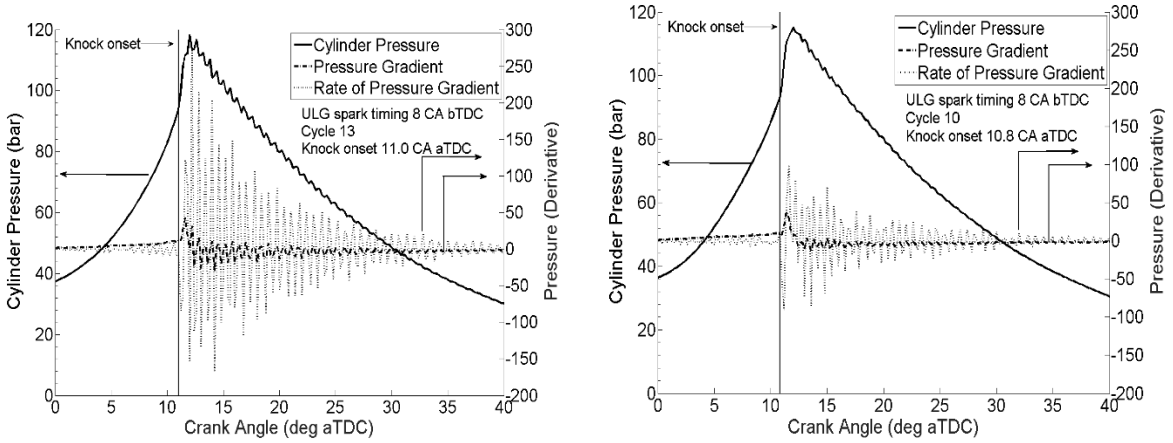

(a) (b)

Figure 3. Typical second and first derivative of pressure computed using the method outlined in Liu[30] superimposed upon the respective knocking cycles of ULG at a spark timing of 8 °CA bTDC (a) cycle number 13 (b) cycle number 10.

3.0 Results and discussion

3.1 Measured combustion characteristics of gasoline, a gasoline/*n*-butanol blend and their surrogates under normal combustion

Figure 4 shows the crank angle resolved cycle-by-cycle pressure traces collected in LUPOE-2D for the four fuel mixtures under normal combustion at a knock-free spark timing of 2 °CA bTDC. Figure 5 presents a comparison of the crank angle resolved mean pressure cycle of each set of 39 pressure cycles shown in Figure 4 for the four fuel mixtures.

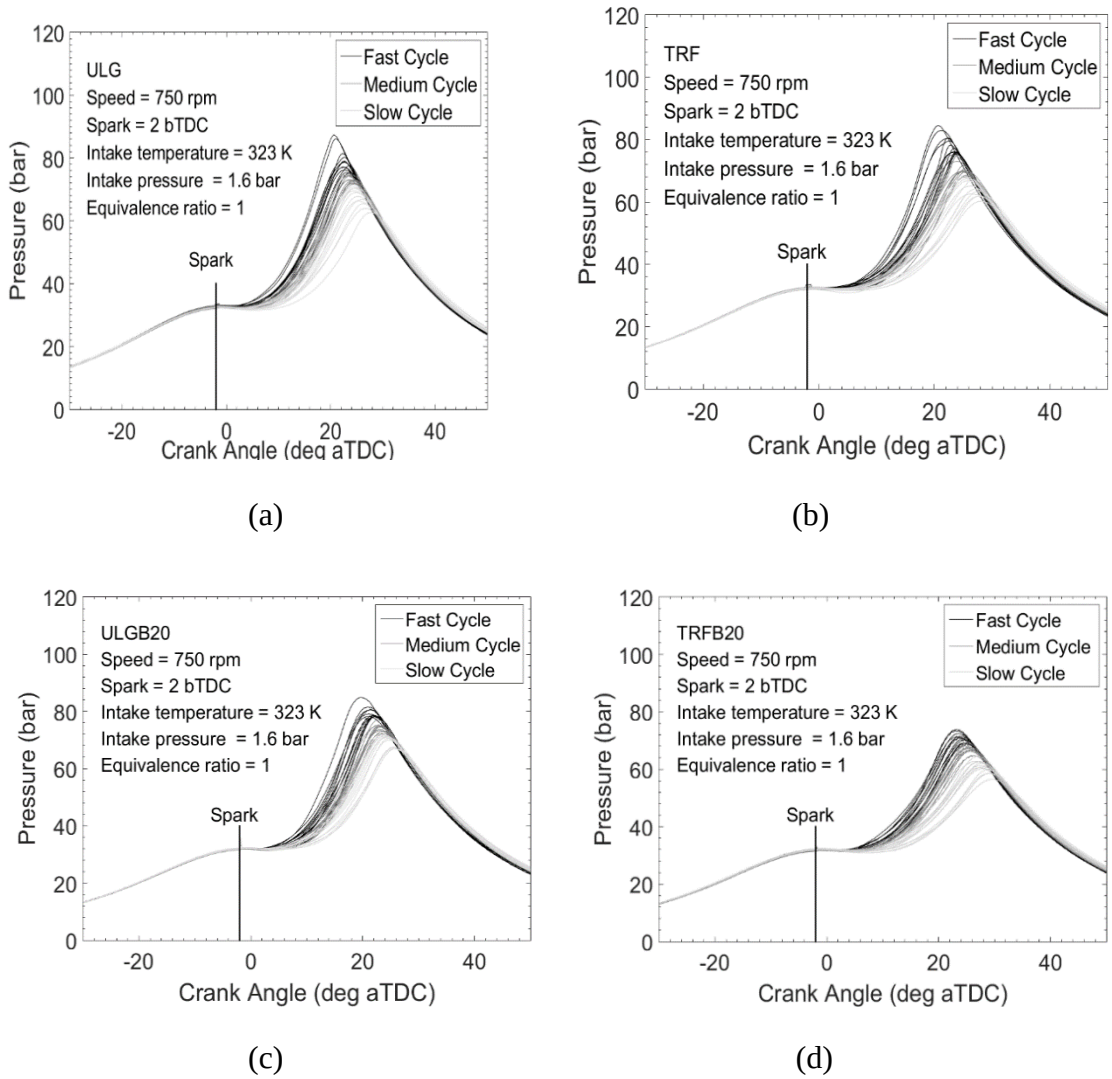

Figure 4. Typical pressure traces collected in LUPOE-2D under normal combustion for the four fuels at a spark timing of 2 °CA bTDC. 39 cycles are shown each for (a) ULG (b) TRF (c) ULGB20 (d) TRFB20.

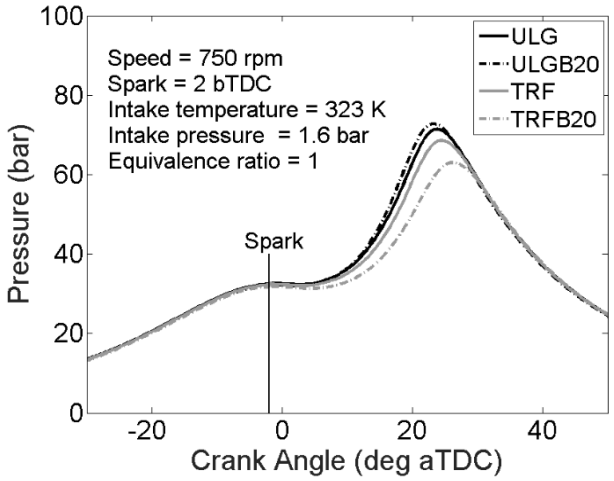

Figure 5. Mean pressure cycles for ULG, TRF, ULGB20 and TRFB20 at a spark timing of 2 °CA bTDC.

Figure 4 clearly shows the magnitude of the cyclic variability in the LUPOE-2D engine which was previously shown[31] to be of a similar magnitude to that found in serial production commercial engines. It is worth emphasising that this variability is an intrinsic characteristic of turbulent combustion: the repeatability of the pressure trace in the motoring cycle in LUPOE-2D is within 2%. In what follows, in addition to analysis of the average, or mean, cycles, distinction is made for statistics of the middle, fast and slow cycles with combustion rates of within one standard deviation of the mean; the mean plus 1.5 times the standard deviation, and the mean minus 1.5 times the standard deviation, respectively.

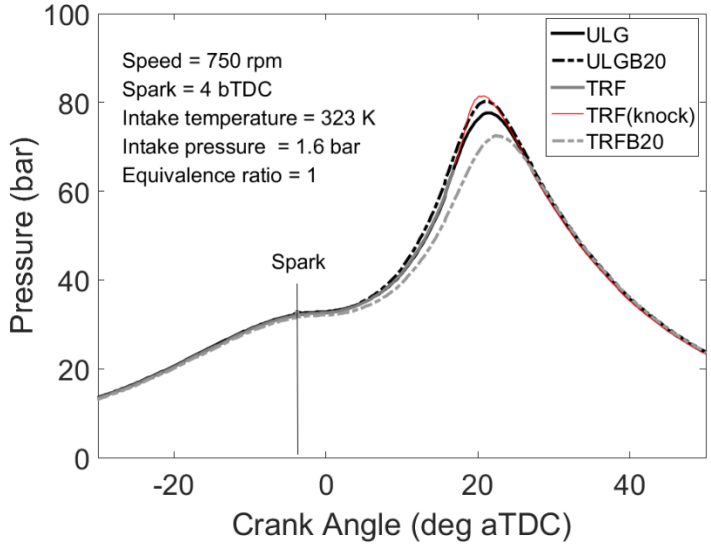

Figure 6. Mean pressure cycles for ULG, TRF, ULGB20 and TRFB20 at a spark timing of 4 °CA bTDC. The thin/coloured parts of the curve indicate the presence of cycles affected by the very fast pressure rise caused by autoignition.

Averaged pressure traces, such as those shown in Figures 5 and 6, were used for autoignition simulations presented in the companion paper in this volume. It should be noted however, that at the spark timing of 4 °CA bTDC, the use of TRF led to autoignition in some fast cycles that was not present for the other fuels under these conditions. The resulting rapid pressure rise led to a high averaged peak pressure as shown in Figure 6 for TRF. The part of the averaged pressure curve affected by auto-ignition in the TRF-air mixtures is shown as a thin/coloured line in Figure 6 and this trace was not used in any subsequent analysis. The pre-ignition averaged pressure traces allow comparison, through thermodynamic modelling,[32, 33] of the

burning rates of the fuels investigated here as shown in Figure 7. It can be seen that although there are some differences between the gasoline and the TRF surrogate, the variability in the turbulent flame speeds of the fuels, which determines the rate of compression of the unburnt charge ahead of the flame, does not exceed 10%. This value is approximately the same as the magnitude of the cyclic variability for an individual fuel, cf. Fig 4.

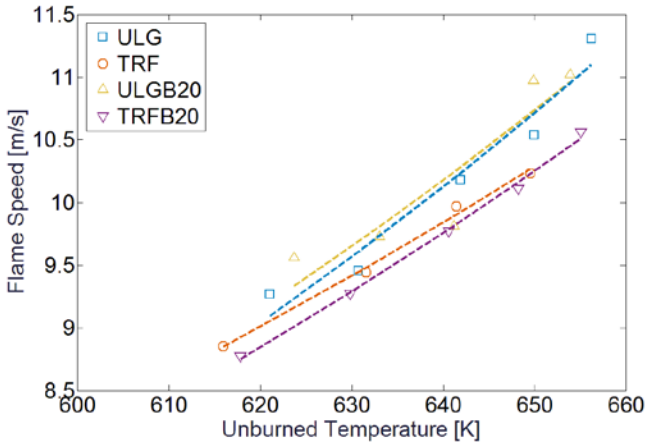

Figure 7. Turbulent flame speeds derived from pressure measurements for the four fuels vs. the unburnt charge temperature.

The peak pressure value is a proxy measure for the burning rate for fuels of comparable calorific value.[22, 25, 34] The 20% *n*-butanol/gasoline blend showed higher burning rates and higher peak pressures compared to gasoline, TRF and the TRF/*n*-butanol blend, see Figures 5 and 7. The faster burning velocity of the gasoline/*n*-butanol blend can be attributed to the impact of the 20% by volume of *n*-butanol in the mixture as alcohols have been generally reported[23, 34] to display higher burning velocities compared to iso-octane and toluene.[35] The TRF surrogate showed slightly lower burning velocities and consequently lower rates of pressure rise compared to the reference gasoline (Figure 7). Looking at the composition of the TRF mixture presented in section 2.4 (Table 2), nearly ninety percent by volume of the mixture comes in the form of the slower burning iso-octane and toluene and this is likely to influence the burning velocity of the TRF as well as the absence of components such as ethanol and olefins which are present in the reference gasoline at about 5 % and 8 % by volume, respectively. However, it may be seen that addition of the *n*-butanol does not change the turbulent flame speed to any appreciable amount, and thus the difference in the knock onset is likely to be attributable to chemical kinetics effects. Investigation of the spark discharge showed that the energy was consistent across the four fuels and therefore is

unlikely to be the cause of any differences in peak pressures. The *n*-butanol has a volumetric combustion enthalpy, approximately 20% lower than any other TRF component and therefore the final pressure at the end of combustion at constant volume will be lower for TRFB20. The decrease in the final pressure in an engine is not linearly proportional to the decrease in calorific value as it is partially offset with faster burning so that the combustion is completed within a smaller volume earlier in the expansion stroke, see Figure 4. For the cycles with a turbulent burning rate that is slower than the average, the combustion ends later in the expansion stroke, see Figure 4d. In this case, peak pressure decreases due to the slightly lower calorific value of TRFB20 and a larger part of the combustion volume becomes significant and affects the average cycles shown in Figures 5 and 6. At a later spark timing of 4 °CA bTDC (Figure 6), the TRF mixture displayed initially a slightly higher burning rate (i.e. higher peak pressure) compared to the other fuel mixtures due to the influence of knock.

Figure 8 presents the cycle-by-cycle analysis of the peak pressures as a function of the crank angle at which they occur at a spark timing of 2 °CA bTDC. In general, the relationship between the measured peak pressures and the crank angle of occurrence is linear across the set of fuels investigated with the higher peak pressures occurring at a corresponding earlier crank angle.[31] It is worth noting that addition of n-butanol to gasoline reduces the magnitude of the cyclic variability in the peak pressure. The averaging of the pressure curves shown in Figs. 5 and 6 is done at a fixed value of the crank angle, and therefore a reduction in the variability will slightly increase the average pressure curve around its peak value adding to the already discussed effects of slightly larger burning velocities.

In order to compare the magnitude of variability in the set of peak pressures collected under normal combustion, the coefficient of variation (COV) of the peak pressure for the 39 cycles recorded at a spark timing of 2 °CA bTDC for each of the four fuels has been computed and is presented in Table 3. The COV is given by the ratio of the standard deviation to the mean of the data. Although the TRF surrogate reproduces the range of peak pressures of the reference gasoline reasonably well as shown in Figure 8, the degree of cyclic variability is higher compared to gasoline, see Table 3. While a higher disparity exists between the ranges of peak pressures measured for the gasoline/*n*-butanol blend and the TRF/*n*-butanol blend (Figure 8), compared to that between gasoline and TRF, the coefficient of cyclic variability (Table 3) between the blends is fairly close. Interestingly, the cyclic variability of the measured peak pressures for the gasoline/*n*-butanol blend and the TRF/*n*-butanol blend are

lower than those of gasoline and TRF respectively (Table 3), indicating the impact of blending on cyclic variability. Minimal cyclic variability is desired in engine operation as a high cyclic variability has the potential to narrow down the engine operating range as well as reduce engine performance.[22, 29]

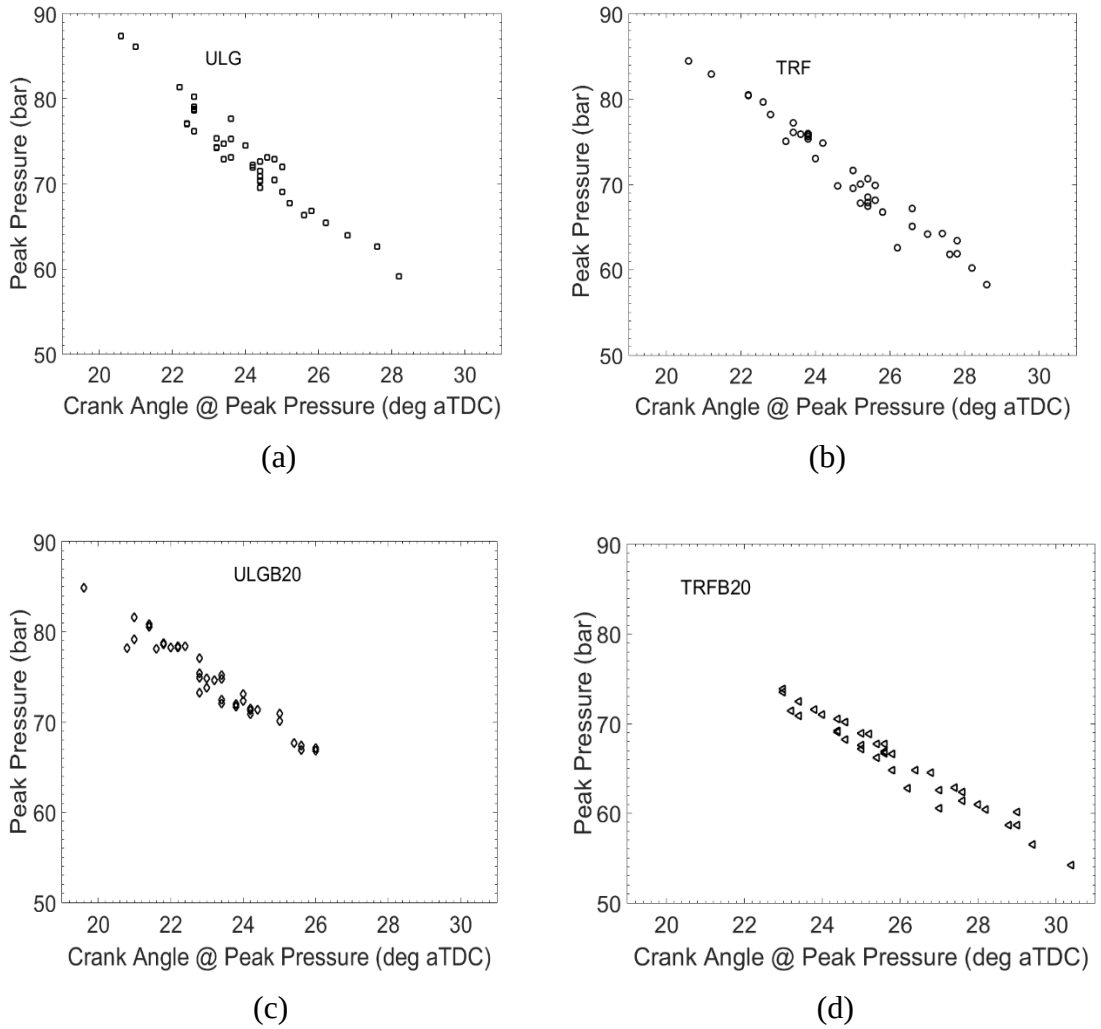

Figure 8. Cyclic variability of peak pressures versus corresponding crank angle at its occurrence measured at a spark timing of 2 ºCA bTDC (a) ULG b) TRF (c) ULGB20 (d) TRFB20.

Table 3: Coefficient of variation of peak pressures for the four fuels at 2 °CA bTDC

Fuel	COV (%)
ULG	7.98
TRF	9.85
ULGB20	6.02
TRFB20	6.87

3.2 Measured combustion properties of gasoline, TRF and their surrogates under knocking conditions

The study of fuel effects on the knock boundary performed for the set of chosen fuels under similar engine conditions and described in section 2.4 showed an earlier knocking regime for the formulated TRF compared to the other three fuels. While gasoline exhibited a similar knock boundary (i.e. spark advance of 6 °CA bTDC), with the blended fuels, for the TRF a knock boundary of 4 °CA bTDC was recorded.

3.2.1 Measured in-cylinder pressures

Typical knocking pressure cycles for the four fuels recorded at a later spark timing of 8 °CA bTDC are presented in Figure 9 while the mean pressures based on the cycles shown in Figure 9 for each of the fuels are compared with one another in Figure 10. Similarly to the the TRF curve in Figure 6, the thin/coloured portions of the curves in Figure 10 show the part of the averaged pressure curves affected by the rapid pressure rise caused by the autoignition of the end gas. One may see that all four mixtures are affected in this case; only the part of the pressure curve shown as a bold line could be used for chemical kinetic simulations. Even though in this case, the peak pressure is no longer a reliable proxy measure of the burning velocity, the latter can be inferred from the rate of the pressure rise prior to knock. Similarly to the results obtained under non-knocking conditions, the gasoline/*n*-butanol blend exhibited the fastest pressure rise and burning velocity with the highest mean pressure while the mean pressure of the TRF/*n*-butanol blend (TRFB20) is lower than that for the rest of the fuels due to a combination of the effects of the slightly lower calorific value of *n*-butanol and a larger cyclic variability resulting in a greater proportion of slow-burning cycles, see Figure 8d and the discussion in section 3.1. Here, we see that at the later spark timing of 8 °CA bTDC, the mean pressure of the TRF mixture (Figure 9 is in very good agreement with that of gasoline and only slightly higher indicating that the disparity between gasoline and the formulated surrogate reduces as the spark timing is well advanced.

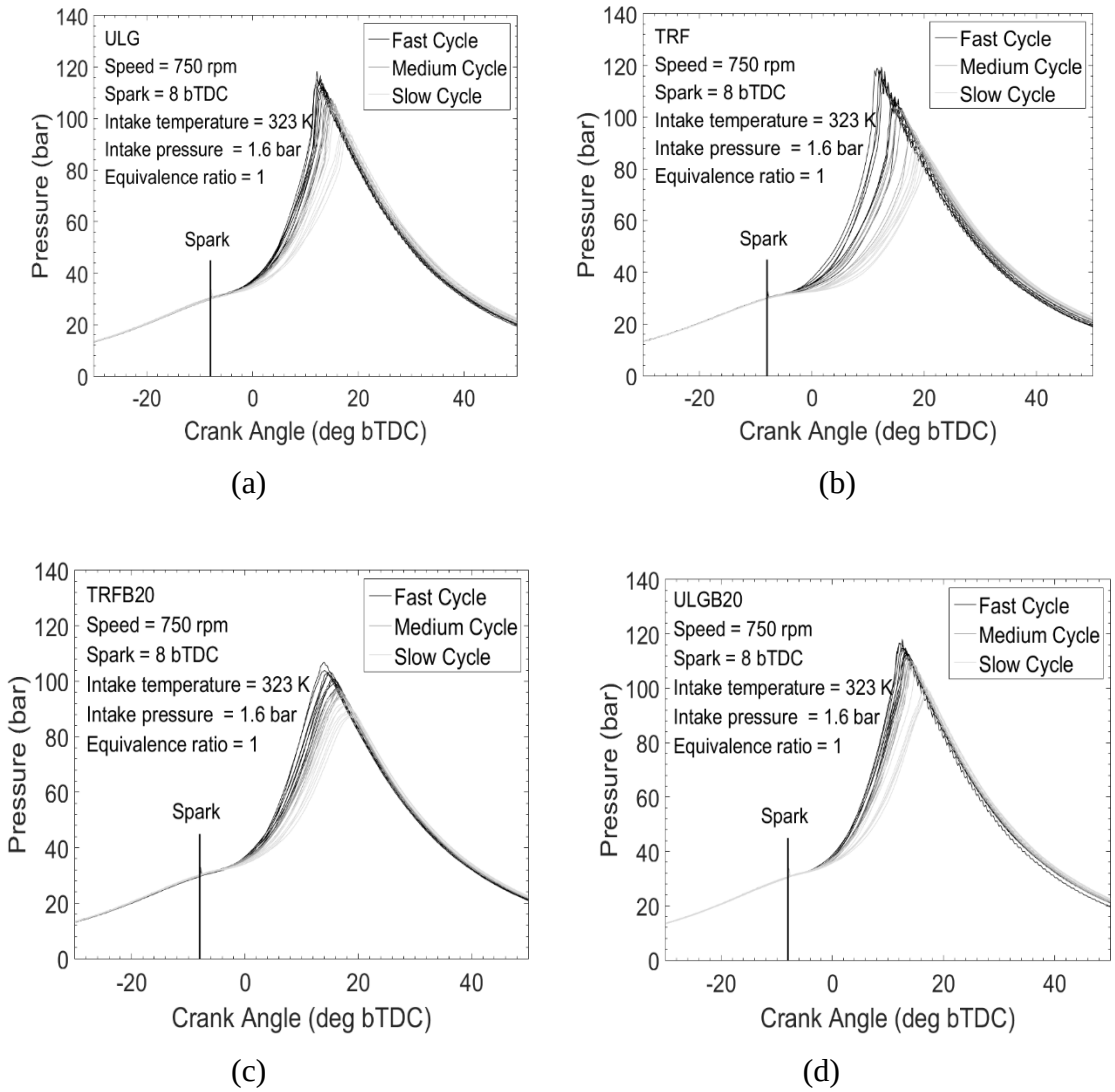

Figure 9. Typical pressure traces collected in LUPOE-2D under knocking combustion for the four fuels at a spark timing of 8 °CA bTDC. Shown are 26 cycles each for (a) ULG (b) TRF (c) TRFB20 and (d) ULGB20.

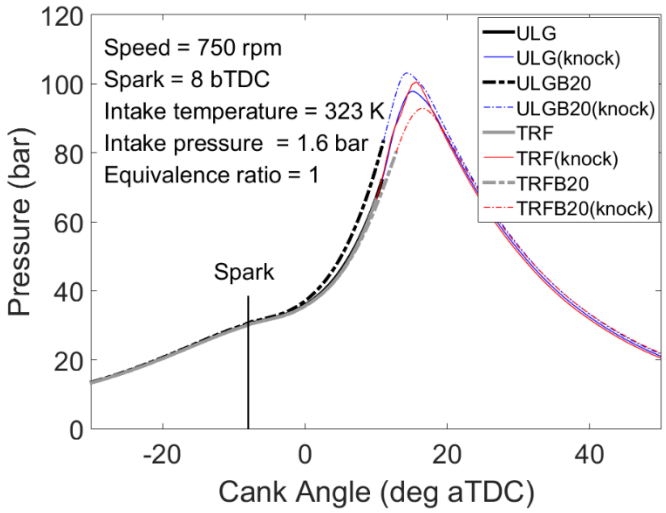

Figure 10. Mean pressure cycles for ULG, TRF, ULGB20 and TRFB20 at spark timing 8 °CA bTDC. The thin/coloured parts of the curve indicate the presence of cycles affected by the very fast pressure rise caused by autoignition.

3.2.2 Measured knock onsets and knock intensities

The knock onsets and knock intensities exhibited by the four fuels across the knocking conditions tested were computed from the measured pressure data using the method described in section 2.6. Figures 11 and 12 show the statistical variation of the knock onsets as well as a comparison of the knock onsets for the four fuels at spark timings of 6 °CA bTDC and 8 °CA bTDC. At a spark timing of 6 °CA bTDC (Figure 11), the TRF fuel knocks earlier than the reference gasoline and blended fuels while the ULGB20 blend knocks slightly later than gasoline (ULG). This indicates that blending an oxygenated fuel such as *n*-butanol with gasoline could possibly lead to improvement in the knocking performance of gasoline. The results obtained here at the later spark timing of 6 °CA shown in Figure 11, are in agreement with the findings within the RCM[26] where, across the temperature range of interest, the ignition delays for TRF are slightly shorter compared to those of the reference gasoline. Similar to the result observed under normal combustion in terms of variation in peak pressures, the spread in knock onset is slightly larger for TRF and slightly smaller for ULGB20 compared to gasoline. At a later spark timing of 8 °CA bTDC (Figure 12) where the in-cylinder pressure and temperature are higher, the TRF also knocks earlier than gasoline, but the difference between the knock onsets of the earliest knocking cycle, as well as the mean knock onsets of both fuels, is considerably smaller compared to that recorded at a spark

timing of 6 °CA bTDC (Figure 11). Whilst temperature measurements were not made in the engine experiments, a parallel modelling study (see companion paper in this volume) indicates temperatures during the early period of the first stage heat release to be ~750 K for the earlier spark timing of 6 °CA and ~800 K for the later spark timing of 8 °CA bTDC. In the RCM study[26], better agreement was obtained for measured ignition delays at around 800 K compared to lower temperatures. Even small differences of 1-2 ms in RCM ignition delays translate into tens of CA degrees difference in knock onset in the SI engine which makes the development of suitable surrogates challenging.

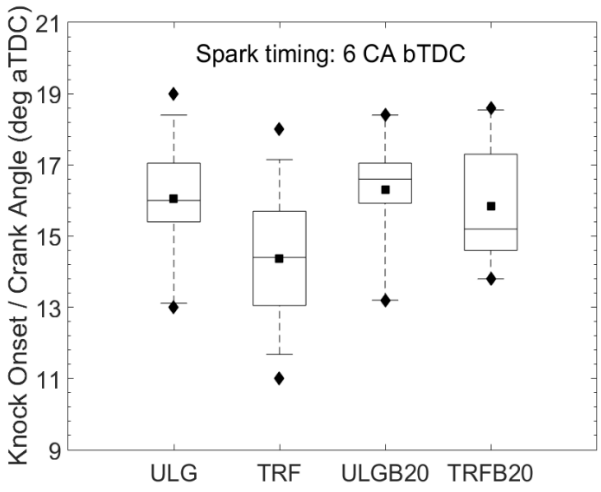

Figure 11. Variation of measured knock onsets across the four fuels tested at 6 °CA bTDC. Boxes represent 25th and 75th percentiles while whiskers represent 5th and 95th percentiles. The squares and horizontal lines represent the mean and median of the measured distribution.

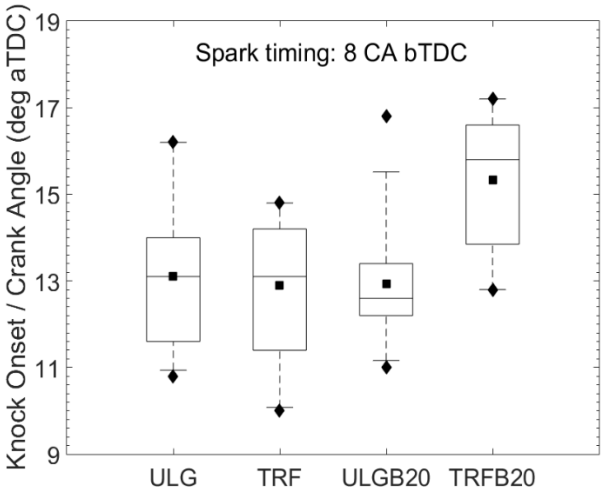

Figure 12. Variation of measured knock onsets across the four fuels tested at 8 °CA bTDC. Boxes represent 25th and 75th percentiles while whiskers represent 5th and 95th percentiles. The squares and horizontal lines represent the mean and median of the measured distribution.

Based on the results obtained in this study, it is clear that compared to gasoline, the formulated TRF would lead to a reduction in the knock limited spark advance (KLSA) as well as a decrease in the power output from the engine. The TRF/*n*-butanol blend gave better agreement with the gasoline blend for the lower temperature conditions at the later spark timing than for the earlier spark timing. Consistent trends between the TRF and gasoline are shown in terms of increasing the CA of knock onset in Figure 11 on the addition of 20% *n*-butanol. This is consistent with the ignition delays measured in Agbro et al.[26] where better agreement between the reference gasoline and formulated TRF was obtained for the blends under lower temperature conditions, where the addition of 20% *n*-butanol increased the ignition delay times. One caveat in comparing the RCM data obtained at 20 bar with the results from the engine studies is of course differences in pre-knock pressures, although the sensitivity analysis carried out for the RCM study highlighted that the main pressure dependent reactions are within the hydrogen kinetic scheme and are not fuel specific. In the higher temperature and NTC region, the addition of 20% *n*-butanol lowered the delay times in the RCM, which is consistent with the trend in the gasoline data at the earlier spark timing seen in Figure 12, but not the TRF data. In the temperature region of 800-850 K, the RCM data show a crossing in the ignition delay curves for the TRF/gasoline and *n*-butanol with the blends sitting in between. Matching the exact cross over temperature of gasoline using the surrogate proved to be difficult and this appears to translate into difficulties in matching the gasoline trends on blending at the more advanced spark timings. Increasing the number of components used in the formulation of the surrogates would be an interesting avenue for further research, with the behaviour of the surrogate in this cross over region of critical importance.

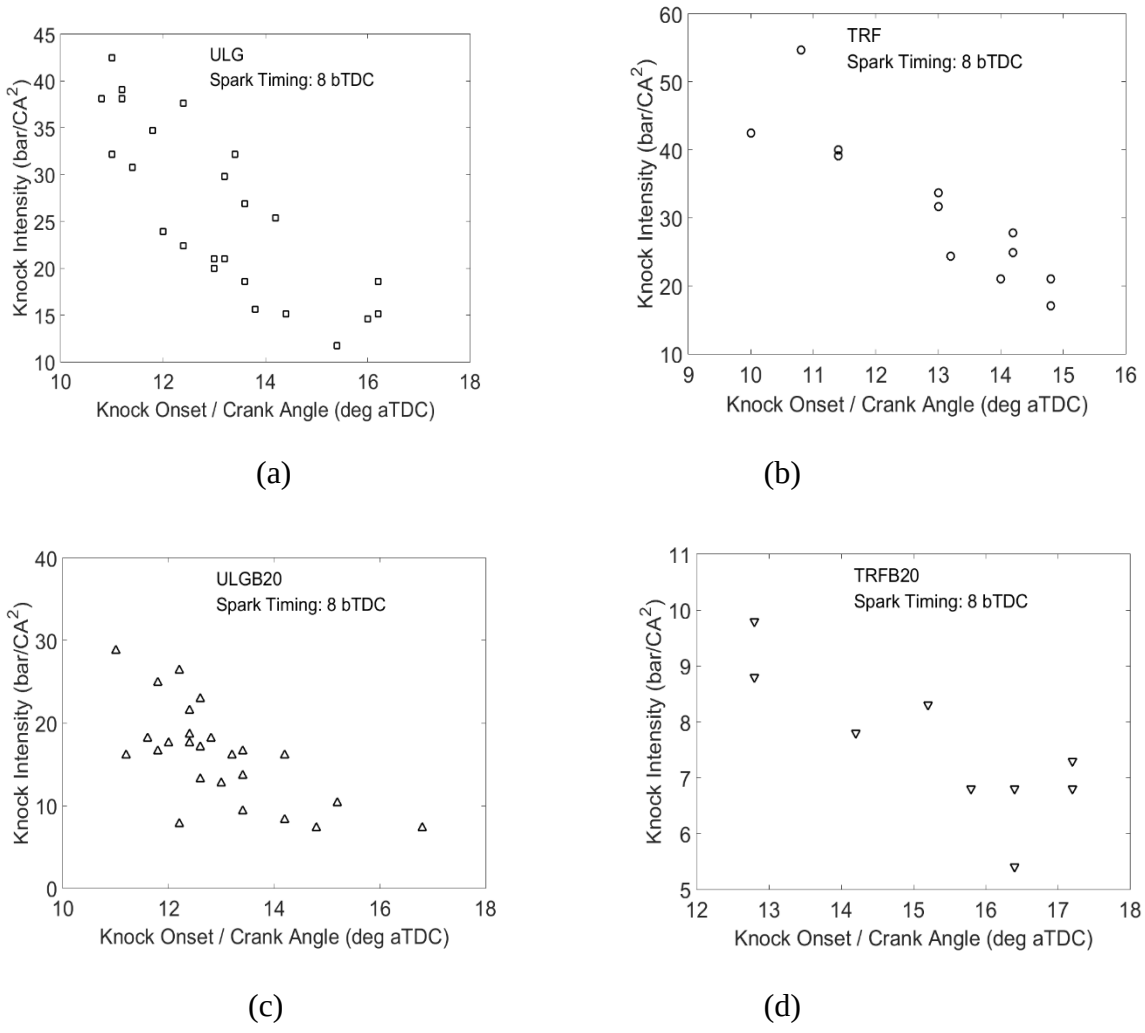

Figure 13. Knock intensities versus corresponding knock onsets of the identified knocking cycle at 8 °CA bTDC (a) ULG (b) TRF (c) ULGB20 (d) TRFB20.

Figure 13 shows an approximately linear relationship between the knock intensity defined by the maximum amplitude of the pressure rise rate, and knock onset, although the data is somewhat scattered. Earlier autoignition leads, as a rule, to more violent pressure oscillations. However, some departure from a strict linear dependency should be expected because the auto-ignition sites appear at random locations,[25] and the location of the auto-ignition site affects the knock amplitude.[8] Figure 14 also depicts a linear relationship between the in-cylinder peak pressures and knock onsets. The level of scatter in the measured knock intensity (Figure 13) is higher than that in the measured peak pressure (Figure 14) and this is due to the difficulty in the analysis of the amplitude of the pressure waves caused by autoignition of the end gas. The addition of *n*-butanol strongly diminishes the knock intensity of the TRF but less so for the gasoline. In both figures, the knock intensity and peak

pressures generally increase as the knock onsets decrease, i.e. as the point of autoignition of the end gas advances towards top the dead centre (TDC). This is understandable since the closer the pressure waves are to the engine top cylinder, the higher the impact (intensity) they are expected to have on the metallic top cylinder surface. Similar to the trend observed for the cyclic variation of peak pressures measured under normal combustion, it is also clear from Figures 13 and 14 that blending leads to a reduction in cyclic variability of measured knock onsets.

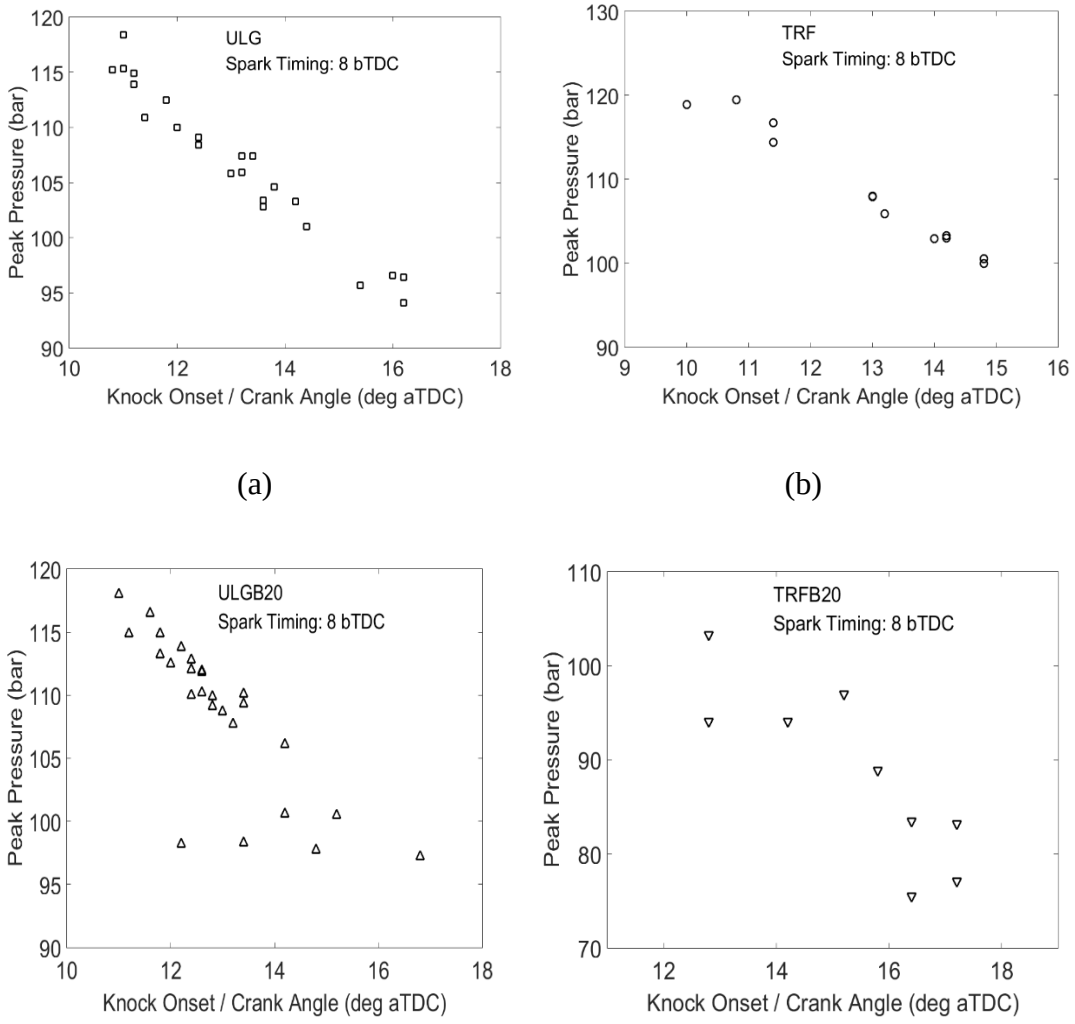

Figure 14. Peak pressures versus corresponding knock onsets of the identified knocking cycles (a) ULG b) TRF (c) ULGB20 (d) TRFB20.

3.2.3 Effect of spark timing on mean peak pressure, knock onset and knock intensities

Figures 15-17 show how the mean values of the peak pressures, knock onsets and knock intensities vary with spark timing across the four sets of fuels. In the test, knock did not occur for the non-TRF fuels at the spark timings of 4 °CA and 5 °CA bTDC and as a result, no data is shown for the non-TRF fuels at those conditions. Also, as mentioned in Section 2.4, no knock data was collected for TRF above the spark timing of 8 °CA bTDC in order to avoid damaging the engine cylinder head due to the excessive in-cylinder pressures developed at those conditions. Across all fuels, delaying the spark timing advances the knock onset location away from TDC (Figure 15) and consequently leads to a reduction in the impact (intensity) of knock (Figure 16). Also, delaying the spark timing leads to a reduction in the in-cylinder peak pressure (Figure 17). However, if the KLSA is later than the maximum brake torque (MBT) timing required to produce the MBT, then the engine performance will be limited by knock. This is where the role of anti-knock fuels such as ULGB20 and TRFB20 becomes very crucial in pushing the spark advance towards the MBT timing while at the same time avoiding the problem of knock. The results shown in Figures 15-17 also clearly indicate that at later spark timings (corresponding to lower temperatures in the engine), the TRF does not seem to be a good representation of gasoline for the pure fuels, possibly reflecting the lower *OI* as shown in Table 2. At the more advanced spark timings, the use of the surrogate TRF tends to exaggerate the effect of butanol in delaying the knock onset.

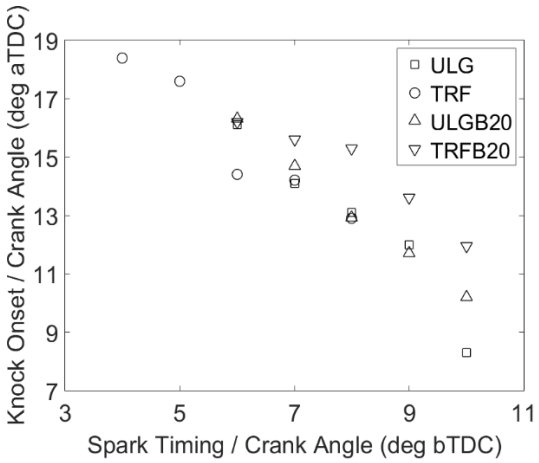

Figure 15. Mean knock onsets at various spark advances (effect of spark timing on mean knock onsets).

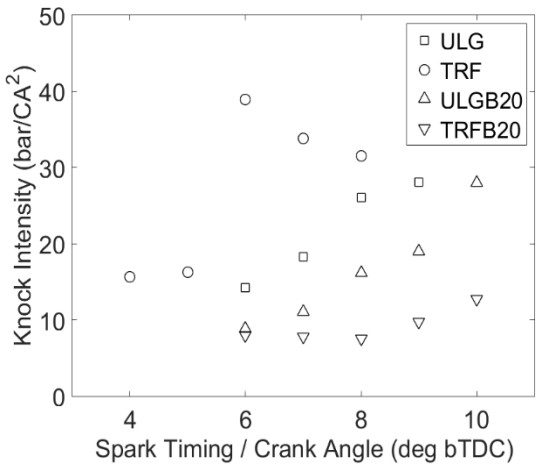

Figure 16. Mean knock intensities (MAPO) at various spark advances (effect of spark timing on knock intensities).

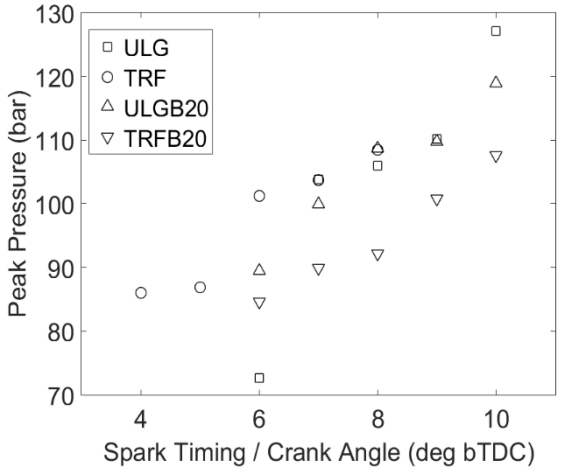

Figure 17. Mean peak pressures at various spark advances (effect of spark timing on mean peak pressures)

4.0 Conclusions

In this work, experimental data of autoignition (knock) onsets and knock intensities of gasoline, a TRF, gasoline/*n*-butanol and TRF/*n*-butanol blends were measured using the Leeds University Optical Engine (LUPOE). The work showed that in contrast to a previous study [26] of ignition delays within an RCM, where the chosen 3-component TRF surrogate was seen to capture the trend of the gasoline data well across the temperature range of 678–858 K, it appears that the chosen TRF may not be an altogether excellent representation of gasoline in the context of simulating combustion under practical engine conditions since the knock boundary of TRF as well as the measured knock onsets at a lower spark timing of 6 °CA which

corresponds to the NTC temperature region of the RCM, are significantly lower than those of gasoline. In this particular study, the use of a three component surrogate allowed the matching of the RON and H/C ratio. In order to allow matching both RON and MON as well as H/C ratio, additional surrogate components would need to be added which adds to the complexity of any potential chemical kinetic mechanism used to simulate the chemical processes occurring in the engine. Should an oxygenate such as ethanol be used as an additional component then the O/C ratio would then also be a target for matching. Developing a more complex surrogate using for example, 5 components, and may improve the agreement with the gasoline data, but this is not a given and would require further study.

Although the gasoline/*n*-butanol blend knocked the latest at the later spark timing of 6 °CA bTDC, its anti-knock enhancing quality on gasoline however disappears at the more extreme (*P*-*T*) conditions of the engine (at later spark timings). Future studies exploring the blending effect of *n*-butanol across a range of blending ratios is required since it is difficult to conclude on the overall effect of *n*-butanol blending on gasoline based on the single blend that has been considered in this study. The study therefore showed that while *n*-butanol holds some promise in terms of its knock resistance performance compared to gasoline, its application as an octane enhancer for gasoline under real engine conditions may be limited.

Acknowledgements

The authors would like to thank Dr. Roger Cracknell and Shell Global Solutions for the provision of fuels. The authors also appreciate the COST (European Cooperation in Science and Technology www.cost.eu) for providing financial support for scientific exchange visits to LOGE Lund Combustion Engineering under the COST Action SMARTCATs (CM 1404). We also thank the Tertiary Education Trust Fund (TETFUND), Nigeria, for scholarship funding for E. Agbro.

References

1. AlRamadan, A. S.; Badra, J.; Javed, T.; Al-Abbad, M.; Bokhumseen, N.; Gaillard, P.; Babiker, H.; Farooq, A.; Sarathy, S. M., Mixed butanols addition to gasoline surrogates: Shock tube ignition delay time measurements and chemical kinetic modeling. *Combustion and Flame* **2015,** 162, (10), 3971-3979.

2. Sarathy, S. M.; Oßwald, P.; Hansen, N.; Kohse-Höinghaus, K., Alcohol combustion chemistry. *Progress in Energy and Combustion Science* **2014,** 44, 40-102.

3. Szwaja, S.; Naber, J. D., Combustion of n-butanol in a spark-ignition IC engine. *Fuel* **2010,** 89, (7), 1573-1582.

4. Kasseris, E. P. Knock Limits in Spark Ignited Direct Injected Engines Using Gasolines/Ethanol Blends. PhD Thesis, Massachusetts Institute of Technology, 2011.

5. Liu, Z. Chemical Kinetics Modelling Study on Fuel Autoignition in Internal Combustion Engines. PhD Thesis, Loughborough University, 2010.

6. Gu, J. Chemical Kinetics Modelling Study of Naturally Aspirated and Boosted SI Engine Flame Propagation and Knock. PhD Thesis, Loughborough University, 2014.

7. Mohamed, C. Autoigntion of Hydrocarbons in Relation to Knock. PhD Thesis, University of Leeds, 1997.

8. Konig, G.; Sheppard, C. *End gas autoignition and knock in a spark ignition engine*; 0148-7191; SAE Technical Paper: 1990.

9. Alasfour, F. N., NOx Emission from a spark ignition engine using 30% Iso-butanol–gasoline blend: Part 1—Preheating inlet air. *Applied Thermal Engineering* **1998,** 18, (5), 245-256.

10. Dernotte, J.; Mounaim-Rousselle, C.; Halter, F.; Seers, P., Evaluation of butanol–gasoline blends in a port fuel-injection, spark-ignition engine. *Oil & Gas Science and Technology–Revue de l'Institut Français du Pétrole* **2009,** 65, (2), 345-351.

11. Gautam, M.; Martin, D., Combustion characteristics of higher-alcohol/gasoline blends. *Proceedings of the Institution of Mechanical Engineers, Part A: Journal of Power and Energy* **2000,** 214, (5), 497-511.

12. Gu, X.; Huang, Z.; Cai, J.; Gong, J.; Wu, X.; Lee, C.-f., Emission characteristics of a spark-ignition engine fuelled with gasoline-n-butanol blends in combination with EGR. *Fuel* **2012,** 93, (0), 611-617.

13. Feng, R.; Yang, J.; Zhang, D.; Deng, B.; Fu, J.; Liu, J.; Liu, X., Experimental study on SI engine fuelled with butanol–gasoline blend and H2O addition. *Energy Conversion and Management* **2013,** 74, (0), 192-200.

14. Wallner, T.; Frazee, R., Study of Regulated and Non-Regulated Emissions from Combustion of Gasoline, Alcohol Fuels and their Blends in a DI-SI Engine. In SAE International: 2010-01-1571; 2010.

15. Williams, J.; Goodfellow, C.; Lance, D.; Ota, A.; Nakata, K.; Kawatake, K.; Bunting, W., Impact of Butanol and Other Bio-Components on the Thermal Efficiency of Prototype and Conventional Engines. In SAE International; 2009-01-1908, 2009.

16. Yang, J.; Yang, X.; Liu, J.; Han, Z.; Zhong, Z., Dyno Test Investigations of Gasoline Engine Fueled with Butanol-Gasoline Blends. In SAE International; 2009-01-1891, 2009.

17. Irimescu, A., Fuel conversion efficiency of a port injection engine fueled with gasoline–isobutanol blends. *Energy* **2011,** 36, (5), 3030-3035.

18. Yacoub, Y.; Bata, R.; Gautam, M., The performance and emission characteristics of C 1-C 5 alcohol-gasoline blends with matched oxygen content in a single-cylinder spark ignition engine. *Proceedings of the Institution of Mechanical Engineers, Part A: Journal of Power and Energy* **1998,** 212, (5), 363-379.

19. Tornatore, C.; Marchitto, L.; Mazzei, A.; Valentino, G.; Corcione, F. E.; Merola, S. S., Effect of butanol blend on in-cylinder combustion process part 2: compression ignition engine. *Journal of KONES Powertrain and Transport* **2011,** 18, (2), 473-483.

20. Wallner, T.; Miers, S. A.; McConnell, S., A comparison of ethanol and butanol as oxygenates using a direct-injection, spark-ignition (DISI) engine. *J. Eng. Gas Turbines Power* **2009,** 131, (ANL/ES/CP-61317).

21. Deng, B.; Yang, J.; Zhang, D.; Feng, R.; Fu, J.; Liu, J.; Li, K.; Liu, X., The challenges and strategies of butanol application in conventional engines: The sensitivity study of ignition and valve timing. *Applied Energy* **2013,** 108, (0), 248-260.

22. Khan, A. F. Chemical Kinetics Modelling of Combustion Processes in SI Engines. PhD Thesis, The University of Leeds, 2014.

23. F. Khan, A.; Burluka, A.; Neumeister, J.; OudeNijeweme, D.; Freeland, P.; Mitcalf, J., *Combustion and Autoignition Modelling in a Turbocharged SI Engine*. 2016; Vol. 9.

24. Roberts, P. a. S., C., The Influence of Residual Gas NO Content on Knock Onset of Iso-Octane, PRF, TRF and ULG Mixtures in SI Engines. *SAE Int. J. Engines* **2013,** 6, (4), 2028-2043.

25. Ling, Z. Flame Propagation and Autoignition in a High Pressure Optical Engine. PhD Thesis, University of Leeds, 2014.

26. Agbro, E.; Tomlin, A. S.; Lawes, M.; Park, S.; Sarathy, S. M., The influence of n-butanol blending on the ignition delay times of gasoline and its surrogate at high pressures. *Fuel* **2017,** 187, 211-219.

27. Kalghatgi, G., *Fuel Anti-knock Quality - Part I, Engine studies*. In SAE International: 2001; 2001-01-3584.

28. Abdi Aghdam, E.; Burluka, A.; Hattrell, T.; Liu, K.; Sheppard, C. G. W.; Neumeister, J.; Crundwell, N., *Study of Cyclic Variation in an SI Engine Using Quasi-Dimensional Combustion Model*. SAE Technical Paper 2007-01-0939, 2007.

29. Heywood, J. B., Fundamentals of internal combustion engines. *NY: McGraw Hill* **1988**, 619.

30. Liu, Z.; Chen, R., A zero-dimensional combustion model with reduced kinetics for SI engine knock simulation. *Combustion Science and Technology* **2009,** 181, (6), 828-852.

31. Burluka, A. A.; El-Dein Hussin, A. M. T. A.; Ling, Z. Y.; Sheppard, C. G. W., Effects of large-scale turbulence on cyclic variability in spark-ignition engine. *Experimental Thermal and Fluid Science* **2012,** 43, 13-22.

32. Liu, K.; Burluka, A. A.; Sheppard, C. G. W., Turbulent flame and mass burning rate in a spark ignition engine. *Fuel* **2013,** 107, 202-208.

33. Burluka, A. A., Combustion in a Spark Ignition Engine. *in: M. Lackner, F. Winter and A.K. Agarwal (Eds.) Handbook of Combustion, vol. 3: Gaseous and Liquid Fuels,* **2010**, 389-414, WILEY-VCH Verlag, Weinheim.

34. Ling, Z.; Burluka, A.; Azimov, U., Knock Properties of Oxygenated Blends in Strongly Charged and Variable Compression Ratio Engines. SAE Technical Paper 2014-01-2608, **2014**.

35. Al-Mughanam, T. Fundamental Characterisation of the Flame Propagation of Synthetic Fuels. PhD Thesis, The University of Leeds, 2013.